Clim. Past Discuss., https://doi.org/10.5194/cp-2018-73
Manuscript under review for journal Clim. Past
Discussion started: 4 July 2018

Late Miocene-Pliocene climate evolution recorded by the red clay covered on the Xiaoshuizi planation surface, NE Tibetan Plateau

Xiaomiao Li[1], Tingjiang Peng[1], Zhenhua Ma[1], Meng Li[1], Zhantao Feng[1], Benhong Guo[1], Hao Yu[1], Xiyan Ye[1], Zhengchuang Hui[1], Chunhui Song[2], Jijun Li[1,3]

1. MOE Key Laboratory of Western China's Environmental Systems, College of Earth and Environmental Sciences, Lanzhou University, Lanzhou 730000, China

2. School of Earth Sciences, Key Laboratory of Western China's Mineral Resources of Gansu Province, Lanzhou University, Lanzhou 730000, China

3. College of Geography Science, Nanjing Normal University, Nanjing 210023,China

*Corresponding author: Key Laboratory of Western China's Environmental Systems (Ministry of Education), College of Earth and Environmental Science, Lanzhou University, Lanzhou 730000, China; *E-mail address*: lijj@lzu.edu.cn(J.J. Li), *Fax*: +86-931-891-2724; *Tel.:* +86-931-891-2724

Abstract

As an analogue for predicting the future climate, Pliocene climate and its driving mechanism attract much attention for a long time. Late Miocene-Pliocene red clay sequence on the main Chinese Loess Plateau (CLP) has been widely applied to reconstruct the history of interior aridification and Asian monsoon climate. However, the typical red clay sequences deposited on the planation surface of Tibetan Plateau are rare. Recently, continuous red clay has been found on the uplifted Xiaoshuizi peneplain in the Maxian Mountains, northeastern (NE) Tibetan Plateau (TP). To reconstruct the late Miocene-early Pliocene climate history of NE Tibetan Plateau and to assess the regional differences between the central and western CLP, multiple climatic proxies were analyzed from the Xiaoshuizi red clay sequence. Our results demonstrate the minimal weathering and pedogenesis from 6.7 to 4.8 Ma, which implicates that the climate was sustained arid. We speculate that precipitation delivered by the paleo-Asian Summer Monsoon (ASM) was limited during this period, and instead the intensification of the westerlies circulation resulted in arid condition in the study region. Subsequently, enhanced weathering and pedogenesis occurred during the interval of 4.8-3.6 Ma, which attests to increasing effective moisture. Thus, we ascribe the obvious arid-humid climate transition near 4.8 Ma to the palaeo-ASM expansion. Increasing Arctic temperatures, the vast poleward expansion of the tropical warm pool into the subtropical regions and water freshening in the subtropical Pacific in response to the closure of the Panamanian Seaway may have been responsible for the thermodynamical enhancement of the palaeo-ASM system, which permitted more moisture to be carried to the NE Tibetan Plateau.

Keywords: Late Miocene-earlyPliocene; Xiaoshui Peneplain; Red Clay; Palaeo-ASM;

Westerly Circulation

1. Introduction

The Pliocene, including the Zanclean (5.33-3.60 Ma) and Piacenzian (3.60-2.58 Ma) stages, is one of the most intensively studied intervals of the pre-Quaternary. The Zanclean climate was generally warm and wet and it is analogous to the present day in terms of (i) land-sea distribution, (ii) orbital configuration, (iii) carbon dioxide levels ranging from 280-380 ppm (Raymo et al., 1996; Fedorov et al., 2013), and (iv) comparable temperatures in the tropic region. In addition, both the Holocene and Zanclean are transitional periods from cold to warm climatic condition. For these reasons, the early Pliocene climate is often used as an analogue for that of the Holocene and attracts much attention. On the other hand, Zanclean is unique and some crucial transitions of the thermorhaline and atmospheric circulation towards modern conditions were undergoing. Temperatures at the high northern latitudes were considerably higher and therefore continental glaciers were almost absent from the Northern Hemisphere (Ballantyne et al., 2010; Dowsett et al., 2010). The warm and wet climate prevailed across the major continents and the warm Arctic is thought to have resulted from a greenhouse effect caused by higher atmospheric moisture content (Abbot and Tziperman, 2008). The low meridional surface temperature gradient resulted in an "equable" climate during this interval (Abbot and Tziperman., 2008; Fedorov et al., 2013). The east-west sea surface temperature gradient in the tropical Pacific during this interval is also believed to be low, which is tightly linked with El Nino Southern Oscillation (Lawrence et al., 2006). However, debate persists on whether permanent El Nino–like conditions were sustained during the Pliocene (Wara et al., 2005; Watanabe et al., 2011; Zhang et al., 2014). Meanwhile, the most significant tectonic movements were the uplift of the TP (Li et al., 2015; Zheng et al., 2000 ; Fang et al., 2005a, 2005b) and gradual closing of the Panama seaway (Lunt et al., 2008; Haug et al., 1998, 2005). These tectonic movements resulted in major changes in the global thermohaline and atmospheric circulation system which were thought to make crucial preconditions for both appearing of ice sheet in northern hemisphere at ~3Ma (Haug et al., 1998; Driscoll et al., 1998) and development of modern east-west hydrographic gradient in the equatorial Pacific (Lawrence et al., 2006; Chaisson et al., 2000).

The ASM and meridional (westerlies) circulation systems, as major components of atmospheric circulation, delivered moisture to Eurasia which might have prepared enough moisture for long-term growth of ice sheet in northern hemisphere between 3 and 2 Ma (Driscoll et al., 1998). Make clear the evolution of the palaeo-ASM and westerlies during early Pliocene is critical to understanding formation mechanism of ice sheet at the Northern high latitudes. Furthermore, the palaeo-ASM might be dynamically linked with the TP uplift, changes in latitudinal and longitudinal heat gradients, global temperature and ice volume during early Pliocene. Warm and wet climate background tends to yield wet climate condition while reductions in the east-west sea surface temperature (SST) gradient in the tropical Pacific results in a weakened summer monsoon (Wang et al., 2000). Several studies have shown that a major atmospheric teleconnection links the ASM with both Arctic volume and the TP uplift (Ding et al., 1990; Li et al., 1991; An et al., 2001; Clift et al., 2008; Sun et al., 2015). Thus, it is crucial to make clear what the climate was like in East Asia under such warm and equable climatic conditions in the Northern Hemisphere.

Previous research has revealed that since the late Miocene, red clay widely deposited across the CLP, indicating that the onset of interior Asian aridification related to the uplift of the TP occurred (Guo et al., 2001; Song et al., 2007; An et al., 2014; Ao et al., 2016; Li et al., 2017). Element, strata and pollen evidence from the Qaidam and Tarim basin demonstrated that the aridification had intensified since early Pliocene (Fang et al., 2008; Sun et al., 2006a, 2017; Chang et al., 2013; Liu et al., 2014). In eastern and central CLP, palaeontological evidence, mineral magnetic parameters and geochemical records from the red clay also indicate a dry climate condition during late Miocene, however, aridification process was interrupted by a long interval of wet climate during the early Pliocene (Wang et al., 2006; Guo et al., 2001; Wu et al., 2006; Song et al., 2007; Sun et al., 2010; Ao et al., 2016). The most controversial climate change occurred during the interval of 4.8-4.1 Ma, for which climate reconstructions from different proxies reveal conflicting palaeoenvironmental trends. For example, field observations and pollen records indicate an intensified monsoon system, but low magnetic susceptibility values are more consistent with arid rather than wet climatic conditions (Ding et al., 2001; Ma et al., 2005; Song et al., 2007; Sun et al., 2010). It's thought to be substantial gleying resulted from large amount precipitation which made magnetic susceptibility invalid over this period (Ding et al., 2001). Obviously, climate changes in westerlies dominated regions and monsoon dominated regions are discrepancy. The inconsistent climate change may be related to different response of westerlies and the palaeo-ASM to global climate changes and the TP uplift during early Pliocene. To clarify the evolution and dynamic of westerlies and the palaeo-ASM, requires accurate paleoclimatic reconstructions in the CLP, especially in the western CLP.

Till now, early Pliocene paleoclimatic records from the western CLP red clay are lacking. Recently, continuous red clay has been found on the uplifted Xiaoshuizi (XSZ) peneplain in the NE Tibetan Plateau and well dated via high-resolution magnetostratigraphy analysis (Li et al., 2017). The special gemorophological and climatic characteristic of the Xiaoshuizi red clay makes it different from the main CLP red clay, and provides particular opportunity to reveal the late Miocene-early Pliocene climate history in NE Tibetan Plateau and discuss the climatic difference between the central and western CLP red clay. In this study, multiple climatic proxies have been applied in the Xiaoshuizi late Miocene-Pliocene red clay sequence. Then we reconstruct the detailed precipitation, chemical weathering and pedogensis history in the Xiaoshuizi planation surface during the interval of 6.7-3.6 Ma. Finally, the regional climate and possible mechanism have been further discussed.

2. Regional background

The XSZ planation surface locates in Yuzhong County in the western Chinese Loess Plateau (Fig. 1). The main XSZ planation surface is at an altitude of 2800 m in the Maxianshan Mountains where it has truncated Precambrian gneiss. The Maxianshan are rejuvenated mountains which protrude into the broad Longzhong Basin, and are in a climatically sensitive zone because of the combined influences of the Asian Monsoon and the northern branch of the mid-latitude westerly circulation system. The planation surface is mantled by over 30 m of loess and over 40 m of red clay. Our previous bio-magnetostratigraphic study has demonstrated that the red clay sequence covered on the XSZ peneplain is dated to ~6.9-3.6 Ma (Li et al., 2017), here we choose the Xiaoshuizi core to

Clim. Past Discuss., https://doi.org/10.5194/cp-2018-73
Manuscript under review for journal Clim. Past
Discussion started: 4 July 2018

discuss the regional climate because of its continuous deposit and whole timescale relative to the Shangyantan core mentioned in Li et al (2017). Yuzhong County lies within the semi-arid temperate climate zone at the junction of the eastern monsoon area, the arid area of northwest china, and the Tibetan Plateau cold region. The East Asian Monsoon system and the westerly circulation operate together. The mean annual temperature is about 6.7 ℃ and the precipitation amount is 300-800 mm. The spatial distribution of precipitation is uneven, decreasing from south to north in Yuzhong County. Precipitation amount increases with elevation at a rate of 27 mm per 100 m, attaining a maximum of 800 mm.

3. Material and methods

The XSZ core (35.81154 °N； 103.8623 °E and 2758.1 m above sea level) is composed of 42 m of pure red clay and ~3 m of red clay with an increasing angular gravel content. The red clay is composed of brownish red and yellowish clay layers. The upper 20 m is impregnated with many horizontal carbonate nodule horizons and most of these horizons underline the brownish red layer; there are occasional carbonized plant root channels, elliptical worm burrows and snail fossil fragments. Fe-Mn stains are more frequent in the brownish layers than in the yellowish layers, which is also the case for horizons containing carbonized root channels. The red clay over the Xiaoshuizi planation surface is similar to that of typical eolian red clay in the CLP, all of which are characterized by many carbonate nodule-rich horizons. Grain-size, carbonate content and magnetic susceptibility samples were taken at 5-cm intervals, while samples for geochemical analysis were collected at 25-cm intervals. Each sample age was modeled using linear interpolation to derive absolute ages, constrained by our previous magnetostratigraphy study. The grain-size distribution of samples was measured with a Malvern Mastersizer 2000 with a detection range of 0.02-2000μm. Magnetic susceptibility (χ) was measured using a Bartington MS2 meter and MS2B dual-frequency sensor at two frequencies (470 Hz and 4700 Hz, designated χ_{lf} and χ_{hf}, respectively). Three measurements were made at each frequency and the final results were averaged. The frequency-dependent magnetic susceptibility (χ_{fd}) was calculated as $\chi_{lf}-\chi_{hf}$. Chemical composition was measured using Panalytical Magix PW2403. The sample preparation procedure for XRF analysis was as follows: first, the bulk sample was heated to 35℃ for 7 days, then each sample was ground to less than 75μm using an agate mortar, and finally about 4 g of powdered sample was pressed into a pellet with a borate coating using a semiautomatic oil-hydraulic laboratory press (model YYJ-40). All the measurements were finished in the MOE Key Laboratory of Western China's Environmental Systems, Lanzhou University. The molar content of silicate Ca (CaO*) was calculated using the following equation:

$$CaO^*(mol) = CaO(mol) - CaCO_3(mol) - \frac{10}{3} * \frac{P_2O_5}{M(P_2O_5)}$$

The carbonate content was measured with a calcimeter using the volumetric method of Avery and Bascomb (1974) in the Key Laboratory of Mineral Resources in Western China (Gansu Province), Lanzhou University.

4. Results

Carbonate content

According to the fluctuations in carbonate content, the red clay sequence was divided into two intervals: *Interval* - Ⅰ is from 6.7-4.8 Ma, during which the carbonate content

Clim. Past Discuss., https://doi.org/10.5194/cp-2018-73
Manuscript under review for journal Clim. Past
Discussion started: 4 July 2018

fluctuates from 3.8-39.2% with an average of 17.4%; the amplitude of fluctuations is small and the carbonate content decreases upwards. From 5.4-4.9 Ma, the carbonate content fluctuations are of greater amplitude than during 6.7-5.4 Ma. *Interval - II* is from 4.8-3.6 Ma, during which the carbonate content fluctuates from 1.6-39.1% with an average of 13.8%. From 4.8-3.9 Ma there are several leaching-accumulation layers with <7% carbonate content in the leached loess layers and >20% carbonate content in the accumulation layers.

Element geochemistry

The XSZ red clay consists mainly of SiO_2, Al_2O_3, CaO and Fe_2O_3 with low concentrations (<5%) of MgO, K_2O, Na_2O, Sr, Rb and Ba (Table 1). The variations in Al_2O_3 and K_2O are synchronous and roughly opposite to that of CaO. The variations in CaO show the same trend as carbonate content. When the carbonate content is high, CaO is high, while Al_2O_3 and K_2O are low. The contents of Al_2O_3 and K_2O from 4.8-3.6 Ma are clearly higher than those from 6.7-4.8 Ma. The variations in these element concentrations from 4.8-3.6 Ma are also greater than those from 6.7-4.8 Ma. The changes in Sr are similar to those of CaO, but opposite to those of Ba and Rb.

Magnetic susceptibility

During interval I (6.9-4.8 Ma), χ_{hf} changes from 9.6-33.3×10^{-8} m^3/kg with an average of 19.4×$10^{-8}$$m^3/kg$. χ_{lf} ranges from 11.4-36.1×10^{-8} m^3/kg with an average of 20.3×10^{-8} m^3/kg, whilst χ_{fd} fluctuates from 0-2.8×10^{-8} m^3/kg with an average of 1.0×10^{-8} m^3/kg. During interval II (4.8-3.58 Ma), χ_{hf} ranges from 12.8-53.9×10^{-8} m^3/kg with an average of 25.4×10^{-8} m^3/kg, χ_{lf} ranges from 13.56-59.0×10^{-8} m^3/kg with an average of 26.9×10^{-8} m^3/kg and χ_{fd} ranges from 0-4.7×10^{-8} m^3/kg with an average of 1.2×10^{-8} m^3/kg. Clearly, the average values of the three parameters are larger during interval Ⅱ than during interval Ⅰ; the amplitudes and durations of the fluctuations of the three parameters during interval Ⅱ are also larger and longer than those during the interval Ⅰ. From 4.8-4.7 Ma, 4.6-4.25 Ma and from 4.1-3.9 Ma, the values of the three parameters are high, and they exhibit peaks from 4.6-4.25 Ma.

Grain-size analysis

The average clay content (<2μm) is 8.2% during interval Ⅰ and 8.0% during interval Ⅱ. The fluctuations in clay content are minor, except for maxima at about 5 Ma, 4.6 Ma and 4.2 Ma. The coarse silt component (>43μm), mainly carried by the East Asian Winter Monsoon, exhibits a different trend to that of the clay content. From 6.7-4.8 Ma, the >43μm curve is characterized by low values and high-frequency fluctuations, while after 4.8 Ma it exhibits high values and long-duration fluctuations.

5. Discussion

5.1 Paleoenvironmental explanation of the proxies

The carbonate content of aeolian sediments is sensitive to varying climatic conditions, and can be readily remobilized and deposited. Previous studies demonstrated that carbonate in the loess-red clay sequence on the CLP records varies with precipitation (Fang et al., 1999; Sun et al., 2010). The carbonate is mainly derived from a mixture of airborne dusts (Fang et al., 1999). Soil micromorphological evidence from the Lanzhou loess demonstrates that carbonate grains in loess are little altered, while those in the palaeosols have undergone a reduction in size as a result of leaching and reprecipitation in the lower Bk horizons as secondary carbonate (Fang et al., 1994, 1999). Furthermore, seasonal alternations between

Clim. Past Discuss., https://doi.org/10.5194/cp-2018-73
Manuscript under review for journal Clim. Past
Discussion started: 4 July 2018

wet and dry conditions are thought to be a key factor in driving carbonate dissolution and reprecipitation (Sun et al., 2010). Thus, changes in carbonate content are generally controlled by the effective precipitation. When effective precipitation is high, carbonate leaching increases, and vice versa. So the carbonate content is regarded as an effective precipitation proxy for studying wet-dry oscillations as well as summer monsoon evolution (Fang et al., 1999; Sun et al., 2010).

Chemical weathering intensity is generally evaluated by the ratio of mobile (i.e., K, Ca, Sr and Na) to non-mobile elements (e.g., Al and Rb). In general, Sr shows analogous geochemical behavior to Ca and is easily released into solution and mobilized in the course of weathering, while Rb is relatively immobile under moderate weathering conditions due to strong adsorption to clay minerals (Nesbitt et al., 1980; Liu et al., 1993). Thus, the Rb/Sr ratio potentially reflects chemical weathering intensity. However, the initial Rb/Sr ratio can be affected by the precipitation of secondary carbonate leached from overlying sediments during pedogenesis (Chang et al., 2013; Buggle et al., 2011), which may limit its environmental significance. The correlation between Sr and CaO* (silicate CaO) is significant in the XSZ section, while the correlation between Sr and $CaCO_3$ is not significant (99% confidence interval). Thus we speculate that the Rb/Sr ratio mainly reflects the weathering intensity in our studied samples (Fig. 4 e and f). In addition, previous study has proposed that the K_2O/Al_2O_3 ratio can also indicate the weathering intensity. Al_2O_3 is typically chosen to measure the mobility of elements due to its high stability (Taylor et al., 1983), while K_2O (mainly produced by the physical weathering of potash feldspar) is easily leached from primary minerals and then absorbed by secondary clay minerals with ongoing weathering

Clim. Past Discuss., https://doi.org/10.5194/cp-2018-73
Manuscript under review for journal Clim. Past
Discussion started: 4 July 2018

(Yang et al., 2006; Liang et al., 2013). In the arid and semi-arid regions of Asia, K_2O is enriched in palaeosols compared to loess horizons (Yang et al., 2006), meaning that the enrichment of K_2O is positively related with the amount of secondary clay. Thus, to some extent, K_2O/Al_2O_3 reflects the amount of secondary clay and hence weathering intensity. Generally, the K_2O/Na_2O ratio is used to evaluate the clay content in loess and is also a measure of plagioclase weathering, avoiding biases due to uncertainties in separating carbonate Ca from silicate Ca (Liu et al., 1993 ; Buggle et al., 2011). As the product of plagioclase weathering, Na_2O is easily leached by increasing precipitation. As mentioned above, K_2O is easily absorbed by secondary clay particles, meaning that high K_2O/Na_2O ratio is indicative of intense chemical weathering.

In the red clay-loess sequence of the CLP, magnetic parameters and clay (<2 μm) content are well correlated and thus are regarded as the proxies of the ASM strength (Liu et al., 2004). Eolian particles usually have two distinct magnetic components consisting of detrital and pedogenic material (Liu et al., 2004). χ_{lf} can reflect the combined susceptibilityof both two components, but changes in χ_{lf} are dominantly affected by changes in the concentration of pedogenic grains (Liu et al., 2004). Grain size distribution of pedogenic particles confining within the superparamagnetic (SP) and single-domain (SD) grain size has been proven to be steady (Liu et al., 2004, 2005). χ_{fd} can detect superparamagneticminerals produced by pedogenesis and therefore the correlation coefficient between χ_{lf} and χ_{fd} can measure the contribution of SP grains (<0.03 μm for magnetite) to the bulk susceptibility (Liu et al., 2004; Xia et al., 2014). As shown in Figure 4A, χ_{lf} is positively correlated with χ_{fd}, which means that the magnetic susceptibility of the XSZ red clay mostly reflects pedogenic enhancement of the primary eolian ferromagnetic content through the in situ formation of fine-grained ferrimagnetic material. This means that the magnetic susceptibility of the red clay on the XSZ planation surface reflects pedogenic intensity. Both the original and pedogenic magnetic signals can be separated using a simple linear regression method (Liu et al., 2004; Xia et al., 2014). We use this method to extract the original magnetic component (χ_0) and the pedogenic magnetite/maghemite component (χ_{pedo}). In this study, χ_{fd} explains 11% of the susceptibility in terms of pedogenic magnetite/maghemite ($\chi_{pedo} = \chi_{fd} / 0.11$).

Pedogenesis results in enhanced secondary clay formation (Sun et al., 2006); however, not all of the clay particles are derived from in situ pedogenesis, but rather are inherited from aeolian transport and deposition. Clay particles can adhere to coarser silt and sand particles (Sun et al., 2006b). In the western CLP, the coarse silt (>40 μm) content is regarded as a rough proxy for the winter monsoon strength (Wang et al., 2002). Therefore, to eliminate this signal from the primary clay particles, the <2 μm/>40 μm ratio is proposed to evaluate pedogenic intensity. Furthermore, the similarity of the variations between the <2 μm/>40 μm ratio and χ_{pedo} confirms that both proxies are sensitive to pedogenic intensity in the XSZ red clay.

5.2 Time domain and frequency domain analysis of the carbonate content and χ_{pedo}

Power spectral analyses of carbonate content and χ_{pedo} show different dominant cycles (Fig. 5). In detail, χ_{pedo} is concentrated in the eccentricity (100 ky), obliquity (41 ky) and precession (21 ky) bands and another periodicities (71 ky and 27 ky) are also evident. In contrast, the carbonate signal is concentrated in the precession (21 ky) and obliquity (41 ky) bands, but it also exhibits even more prominent periodicities at 56 ky and 30 ky. Furthermore,

Clim. Past Discuss., https://doi.org/10.5194/cp-2018-73
Manuscript under review for journal Clim. Past
Discussion started: 4 July 2018

Morlet wavelet transform analysis of both carbonate content and χ_{pedo} show that the orbital signal increases since 4.8 Ma (Fig. 5 d).

As for the non-orbital cycles, King (1996) proposed that these may possibly originate from harmonics or interactions of the orbital cycles, while Lu (2004) ascribed them to the unstable dust deposition processes followed by varying pedogenesis in palaeosol units. Here we speculate that they may be caused by the low deposition rate, which potentially resulted in the incomplete preservation of the paleoclimatic signal, especially for short cycles of precipitation change. Thus, the incomplete nature of the red clay time series may be responsible for the presence of spurious cycles. In addition, the carbonate content at various depths is affected by leaching which means that the record integrates soil polygenetic processes, thus obscuring orbital forcing trends related to precipitation amount. Low deposition rates, compaction and leaching processes would obscure the orbital cycles, and spectral peaks that do not correspond to orbital cycles may reflect these processes.

To investigate the post-6.7 Ma evolution of the climate signals in the XSZ section in the frequency domain, we filtered the carbonate content and χ_{pedo} time series at the 100, 41, and 21-kyr periods, using Gaussian band filters centered at frequencies of 0.01, 0.02439, and 0.04762, respectively, and compared them with the equivalent filtered components of the stacked deep-sea benthic foraminiferal oxygen isotope record. Our results show that the fluctuations of the three filtered components of both two proxies change rapidly from very low amplitude from 6.7-4.8 Ma to a much larger amplitude from 4.8-4.1 Ma (Fig. 5). The enhanced orbital-scale variability of the two proxies from 4.8-4.1 Ma implies an increased seasonality and wet-dry contrasts. This shift is not observed in the earth orbital parameters but is observed in the filtered 41-kyr component of the stacked deep-sea benthic foraminiferal oxygen isotope record ($\delta^{18}O$). This means that the increased contrast in wet-dry oscillations at the XSZ site was not driven directly by changes in solar radiation intensity but rather was linked with changes in ice volume or global temperature.

5.3 Late Miocene-Pliocene climate history revealed by the Xiaoshuizi red clay

5.3.1 Multiporxy evidence for the dry climate during the interval of 6.7-4.8 Ma

Based on the previous mentioned proxies of pedogenesis and chemical weathering, we reconstruct the late Miocene and early Pliocene climatic history of the Xiaoshuizi peneplain, NE Tibetan Plateau. As shown in Figure 6, we observe that a significant change recorded by the most of the multiproxy (carbonate, Rb/Sr, K_2O/Al_2O_3, χ_{pedo}) occurred near 4.8-4.7 Ma, and therefore the climatic record was generally divided into two intervals. During interval I (6.7-4.8 Ma), the relatively high carbonate values with minor fluctuations indicate that the climate was dry and low Rb/Sr, K_2O/Al_2O_3 and K_2O/Na_2O ratios support the weak chemical weathering. Importantly, both the Rb/Sr and K_2O/Na_2O ratios show opposite trends with carbonate content, meaning that low effective precipitation resulted in weak chemical weathering intensity. Furthermore, the pedogenic proxies (<2 μm/>40 μm ratio, χ_{pedo} and χ_{lf}), which characterised by low values with minor fluctuations, generally supports the weak pedogenesis under the arid climate. Thus, during this interval the Xiaoshuizi climate was relative arid, which characterized by weak chemical weathering and pedogenesis intensity. However, subtle differences exist when these proxies detailed climate changes especially when climate is relative wet. It is evident that the carbonate content decreases with increased variation amplitude after 5.5 Ma, which is consistent with the cycles of carbonate nodules

Clim. Past Discuss., https://doi.org/10.5194/cp-2018-73
Manuscript under review for journal Clim. Past
Discussion started: 4 July 2018

Climate of the Past Discussions Open Access EGU

within paleososol horizons observed in the field (Li et al., 2017). It may be increased precipitation which induced eluviation-redeposition of carbonate since 5.5 Ma. However, from pedogenesis indicies we observe that the general arid climate was interrupted by two enhanced pedogenesis events (occurred at 5.85-5.7 Ma and 5.5-5.35 Ma, respectively). The subtle differences may result from different sensitivity of magnetic susceptibility and carbonate content to precipitation variability when precipitation is low (Sun et al., 2010). In addition, a record of mollusks from the western Liupanshan showed cold-aridiphilous species dominating which also document the cold and dry climate condition on the western CLP during late Miocene (Fig . 7 g).

During this interval, pollen, mollusk and magnetic records from the central and eastern CLP also indicate generally dry and cold climatic conditions (Wang et al., 2006; Wu et al., 2006; Nie et al., 2014). However, the obvious difference is that the Xiaoshuizi arid climate is relative stable, while the climate of central and eastern CLP was interrupted by several obvious humid stages. For instance, two humid stages (6.2-5.8 Ma and 5.4-4.9 Ma) are recorded by the magnetic susceptibility of red clay in the hinterland of the CLP, but are not recorded by the Xiaoshuizi magnetic susceptibility (Fig. 7). It is worth noting that 41-kyr filtered component of thermo-humidiphilous species from the Dongwan was damped in late Miocene (Li et al., 2008). Similarly, the amplitude of the orbital periodicities, filtered from the XSZ carbonate content and χ_{pedo}, are obviously damped from 6.7-4.8 Ma. However, the three periodicities in Summer Monsoon Index from the central CLP show no obvious difference between the late Miocene and Pliocene, but only a slight reduction in variability after 4.2 Ma (Sun et al., 2010). Therefore, we agree that a dry climate prevailed on the CLP during the interval of 6.7-5.2 Ma. The only difference is that the climate in the CLP hinterland fluctuated more significantly than that of the Xiaoshuizi red clay.

The particularly damped response of the western CLP wet-dry oscillations to obliquity forcing may indicate the palaeo-ASM had a negligible influence on the western CLP. It is widely known that the summer monsoon intensity decreased from southeast to northwest across the CLP. A regional climate model experiment demonstrated that the modern Asian summer monsoon was not fully established in the late Miocene and had only a small impact on the northern China (Tang et al., 2011). The weak palaeo-ASM intensity from 7.0-4.8 Ma has been revealed by hematite/goethite and smectite/kaolinite ratios at ODP Site 1148 from the South China Sea (SCS) (Fig 7 i and j). Therefore, we deduce that the Asian monsoon was weak and put a small impact on the Xiaoshuizi climate. In addition, during late Miocene, the TP was not intensively uplifted and thus it could not block the westerlies completely (Li et al., 2015). Previous studies suggested that the red clay may have been transported by both low-level northerly winds and upper-level westerlies (Sun et al., 2004; Vandenberghe et al., 2004). This means the impact of the westerly circulation on the study region cannot be ignored. Notably, pedogenesis proxies roughly parallel to the stacked deep- sea benthic foraminiferal oxygen isotope curve (Fig. 6). It indicates when global temperature was low, pedogenesis intensity increased. It is unreasonable if the precipitation was dominated by the palaeo-ASM. Thus, we speculate from 6.7 to 4.8 Ma, the precipitation transported by the palaeo- ASM was limited and the westerly circulation probably dominated the climate of our study region.

The simultaneous reduction in amplitude of the 41-kyr filtered components from the

Clim. Past Discuss., https://doi.org/10.5194/cp-2018-73
Manuscript under review for journal Clim. Past
Discussion started: 4 July 2018

western CLP and the deep sea $\delta^{18}O$ record from 6.7-4.8 Ma likely indicates that the dry climate was related to changes in global temperature and ice volume. Look around the globe, a cooling climate would be witnessed in late Miocene. $\delta^{18}O$ records from DSDP and ODP sites show an increase of ~1.0‰ during the late Miocene which resulted from the increased ice volume and the associated decrease in global temperature (Zachos et al., 2001). Records from high latitude regions of the northern Hemisphere show continuously decreasing temperatures and increasing ice volume during the late Miocene (Jansen and Sjøholm, 1991; Mudieand Helgason, 1983; Haug et al., 2005). In the Quaternary, the dry climate prevailed during glacial periods when global average temperature (especially in summer) was low. Cool summers would have resulted in a small land-sea thermal contrast which in turn weakened the palaeo-ASM in the late Miocene. Furthermore, the increased ice volume in the Northern Hemisphere resulted in an increased meridional temperature gradient, thus strengthening the westerlies and driving them southward. This would have prevented the northwestward penetration of the Asian Summer Monsoon, which was also proposed as the driving mechanism for a weak EASM in northern China during glacial periods (Sun et al., 2015). Thus, the southward shift of the westerlies had a significant impact on the XSZ region. Global cooling and the growth of polar ice-sheets reduced the amount of atmospheric water vapor; thus, relatively little moisture was carried by the westerlies, producing a dry and stable climate in the XSZ region. In conclusion, global cooling and increasing ice volume in the Northern Hemisphere contributed to dry climatic conditions in the study region.

5.3.2 Humid climate with enhanced fluctuations during the interval of 4.8-3.6 Ma

During interval Ⅱ (4.8-3.6 Ma), the available proxy evidence indicates that the

Xiaoshuizi climate turns into humid condition from previous arid climate. The carbonate content was low on average but with large fluctuations, indicating that the climate was generally humid with increased dry-wet oscillations, especially during the interval of 4.8-3.9 Ma. Several obvious eluvial-illuvial cycles are observed from 4.8 to 3.9 Ma. The carbonate content in the eluvial horizons was less than 10%, whereas in illuvial horizons it exceeded 30% (Fig. 6). The emergence of high frequency cycles of carbonate eluviation-redeposition indicates that seasonal precipitation was increased during this interval. Furthermore, the variations of Rb/Sr and K_2O/Na_2O ratios are very similar to those of carbonate content, which suggests that weathering intensity was related to precipitation amount. Generally, high <2 μm / >40 μm ratio, χ_{pedo} and χ_{lf} correspond to large contrasts in carbonate content between eluvial and illuvial horizons; thus, increased precipitation had a significant influence on enhanced pedogenic intensity. From 4.8 to 3.9 Ma, high precipitation persisted and the weathering and pedogenesis intensity were strong. The K_2O/Al_2O_3 ratio also increased rapidly at about 4.8-4.7 Ma and maintained relatively high values after 4.7 Ma. This may indicate that the overall weathering intensity was sufficient to produce secondary clays, resulting in a spike in K_2O concentration. From 4.60-4.25 Ma, pedogenesis and weathering intensity reach the maximum, as was precipitation intensity, which was manifested by enhanced eluviation and carbonate accumulation. From 3.9 to 3.6Ma, precipitation decreased, and then weathering and pedogensis intensity weakened, which may indicate that the Xiaoshuizi climate is generally humid toward arid direction. Consisting with XSZ records, Dongwan mollusk records also indicate the warm and wet conditions on the western CLP during early Pliocene (Fig. 7 h).

Palynological and terrestrial mollusk records from the central CLP also indicate

Clim. Past Discuss., https://doi.org/10.5194/cp-2018-73
Manuscript under review for journal Clim. Past
Discussion started: 4 July 2018

relatively humid conditions during early Pliocene (Wang et al., 2006； Wu et al., 2006). The magnetic susceptibility records from the CLP hinterland exhibit similar characteristics to the XSZ records that both the magnitude and variability of magnetic susceptibility are large from 4.8-3.6 Ma. From 4.1-3.9 Ma, the enhancement of magnetic susceptibility indicates that humid climatic conditions prevailed across the entire CLP (Fig. 7). Obviously, when precipitation amount peaked from 4.6-4.25 Ma in the XSZ section, the χ_{lf} values at Xifeng, Lingtai and Chaona were low. However, the Lingtai Fe_2O_3 ratio record showed an extraordinary high value corresponding to abundant clay coating over the interval of about 4.8-4.1 Ma and this interval was interpreted as the strongest ASM intensity in the CLP since 7.0 Ma (Ding et al., 2001). In addition, the relative intensity of pedogenic alteration of the grain-size distribution was the strongest during the interval from 4.8-4.2 Ma in the Lingtai section (Sun et al., 2006c). Pollen assemblages at Chaona indicate a considerably warmer and more humid climate from 4.61-4.07 Ma (Ma et al., 2005). These evidences indicate climate from 4.6-4.25 Ma is warm and wet in the central CLP. Gleying has been implicated in reducing the value of magnetic susceptibility as a record of precipitation during this period (Ding et al., 2001). When soil moisture regularly exceeds the critical value, dissolution of ferrimagnetic minerals occurs and the susceptibility signal is negatively correlated with pedogenesis (Liu et al., 2003). This by itself indicates that precipitation was likely to have been very high during this interval.

In summary, a wet climate prevailed across the CLP in early Pliocene. At the same time, hematite/goethite ratio from the SCS also shows enhanced precipitation amount and Smectite/Kaolinite ratio there shows increased seasonality at about 4.8Ma (Fig. 7 i and j), which indicate the enhancement of palaeo-ASM (Clift et al., 2006, 2014). Thus, we regard climate change of Xiaoshuizi as the result of expansion of the Palaeo-ASM expressed in its intensity and reach during this interval.

The remarkably increased amplitude of the 41-kyr filtered components from XSZ and the deep sea $\delta^{18}O$ record at about 4.8 Ma indicates the expansion of palaeo-ASM may be related to changes in global temperature and ice volume. Furthermore, decreasing input of ice raft debris into subarctic northwest Pacific was synchronous with the expansion of palaeo-ASM during early Pliocene (Fig. 6). In addition, from 4.8-4.7 Ma and 4.6-4.25 Ma, the high values of the three pedogenic indices at the XSZ section indicate that strong pedogenic intensity corresponded with high SSTs in the eastern equatorial Pacific (EEP). These coincides imply that phases of enhanced precipitation may be correlated with changes in SST and ice volume (or temperature) at northern high latitudes.

5.4 Possible mechanism for the paleo-ASM expansion during early Pliocene

Ding (2001) proposed that uplift of the TP to a critical elevation resulted in an enhanced summer monsoon system during 4.8-4.1 Ma. The TP uplift was shown to have had profound effects on the ASM initiation, having strengthened ASM intensity and changed the shape of the precipitation band in East Asia (Li et al., 1991, 2014; An et al., 2001). A more detailed modeling study demonstrated that the uplift of the northern TP mainly resulted in an intensified summer monsoon and increased precipitation in northeast Asia (Zhang et al., 2012). From 8.26-4.96 Ma, massive deltaic conglomerates were widely deposited and the sediment deposition rate increased, indicating the uplift of the Qilian Mountains (Song et al., 2001). At the same time, the Laji Mountains underwent a pronounced uplift by thrusting at about 8 Ma, which resulted in the current basin-range pattern (Li et al., 1991; Fang et al., 2005a; Zheng et al., 2000). However, geological and palaeontological records indicate that the uplift of the eastern and northern margins of the TP was very small from late Miocene to middle Pliocene (Li et al., 1991, 2015; Zheng et al., 2000; Fang et al., 2005a, 2005b). So we speculate the TP uplift may be not the major contribution to the expansion of palaeo-ASM occurred at ~4.8 Ma.

As mentioned above, the extremely wet climate across the CLP was synchronous with the gradual closure of the Panama Seaway, which led to a larger reorganization of the global thermohaline circulation pattern. Nie (2014) proposed that the freshening of the Eastern Equatorial and North Pacific surface water, resulting from the closure of the Panama Seaway since 4.8 Ma (Haug et al., 2001), led to sea ice formation in the North Pacific Ocean, which enhanced the high-pressure cell over the Pacific and increased the strength of southerly and southeasterly winds. However, there was a warming trend in the Northern Hemisphere at 4.6 Ma (Haug et al., 2005; Lawrence et al., 2006). The gradual closure of the Panama Seaway resulted in the reorganization of surface currents in the Atlantic Ocean. In particular, the Gulf Stream was enhanced and began to transport warm surface waters to high northern latitudes, thus strengthening the Atlantic meridional overturning circulation and warming the Arctic (Haug et al., 1998, 2005). This in turn resulted in higher global atmospheric water vapor levels which promoted warm moist conditions during the Pliocene (Abbot and Tziperman, 2008; Dowsett et al., 2010). Three independent proxies from an early Pliocene peat deposit in the Canadian High indicate that Arctic temperatures were 19 ℃ warmer during the early Pliocene than at present (Ballantyne et al., 2010). Therefore, even freshening of the Pacific

Clim. Past Discuss., https://doi.org/10.5194/cp-2018-73
Manuscript under review for journal Clim. Past
Discussion started: 4 July 2018

led to sea ice formation in the North Pacific Ocean. However, this process would be delayed (occurring during 3.2-2.7 Ma) and the extent of the sea ice in the early Pliocene was thus very limited. In contrast, the warming of the northern high latitude region led to increases in summer temperature in the mid-latitudes of Eurasia. On the other hand, equatorial SSTs remained stable or cooled slightly (Brierley et al., 2009; Fedorov et al., 2013). This amplified the land-ocean thermal contrast and was essential for enhancing the palaeo-ASM. Furthermore, external heating derived from reduced planetary albedo also enhanced the thermal contrast between the Pacific and Eurasian regions (Dowsett et al., 2010). On the other hand, the unusually warm Arctic and small meridional heat gradient in the Northern Hemisphere pushed the Intertropical Convergence Zone northward. This weakened the westerly circulation and thus facilitated the northwestward expansion of the ASM.

Fig 6 indicated high values of pedogenic indices at the XSZ section correspond with high SSTs in the EEP. It seems to be discrepancy with the modern ENSO cases (when the EEP temperature is high, the precipitation amount of the western CLP is low). The discrepancy may indicate sea-air interaction during early Pliocene is different from today. From 4.8 to 4.0 Ma, the thermahaline circulation was reorganizing and creating a precondition for the development of the modern equatorial Pacific cold tongue (Chaisson et al., 2000). Some crucial changes linked with summer monsoon occurred. We noticed a vast expansion of the western Pacific warm pool into subtropical regions occurred in early Pliocene (Brierley et al., 2009; Fedorov et al., 2013). Temperatures at the edge of the warm pool show a warming trend of ~2℃ from the latest Miocene to the early Pliocene (Karas et al., 2011). The thermal state of the WEP warm pool significantly enhanced the summer monsoon and its northward extension. In modern times, when the north of western pacific warm pool was warm, the convection over and around the Philippine was enhanced. Subsequently, the northern extent of the western Pacific subtropical high shifted northwards from the Yangtze River valley to the Yellow River valley and moisture was introduced across the entire CLP (Wang et al., 2000; Huang et al., 2003). Whether it is also the case for the early Pliocene or not needs further researching. However, warming and freshening seawater of subtropic Pacific would have been more readily evaporated which would have provided enhanced moisture for the palaeo-ASM leading to increased rainfall across the CLP.

Thus, we deduce it may be warming of high northern latitudes, accompanied by the vast poleward expansion of the tropical warm pool into the subtropical regions and freshening of water in the subtropical Pacific facilitated the expansion of the palaeo-ASM during early Pliocene.

6. Conclusions

Continuous late Miocene-Pliocene red clay preserved on the representative planation surface in NE Tibetan Plateau provides particular opportunity to discuss the Asian monsoon history. Multi-proxy records from the XSZ planation surface in the western CLP, together with other palaeoclimatic records from the CLP, reveal two intervals of major climatic change from 6.7 to 3.6 Ma. During the first interval (6.7-4.8 Ma), the XSZ records indicate that both the amount and variability of precipitation were small; however, they were much greater in the hinterland of the CLP. Thus, the palaeo-ASM had little influence on the climate of the western CLP during this interval. During the second interval (4.8-3.6 Ma), the XSZ records indicate that both the amount and variability of precipitation were large. From 4.8 and 3.6 Ma, the climate was characterized by abrupt increases in the seasonality of precipitation, which attests to a major northwestward extension and enhancement of the summer monsoon. Obviously, multiple paleoclimatic proxies show that the strongest summer monsoon occurred during the interval of 4.6-4.25 Ma. The expansion of palaeo-ASM may have been caused by warming of the Arctic, the vast poleward expansion of the tropical warm pool into the subtropical regions and freshening of water in the subtropical Pacific in response to the closure of the Panamanian Seaway during early Pliocene.

Author contribution: Tingjiang Peng and Jijun Li supported fund and edited the article. Zhenhua Ma provided age frame and participated in the most of field work. Meng Li, Zhantao Feng, Benhong Guo, Xiyan Ye and Hao Yu participated in investigation and experiment works. Chunhui Song and Zhengchuang guided and supervised the field work.

Competing interests: The authors declare that they have no conflict of interest.

Acknowledgements

We thank Ai Song for the field drilling and Fengxia Yu for her early experimental work. This work was supported by National Natural Science Foundation of China (41330745, 41401214) and Key Laboratory of Continental Collision and Plateau Uplift, Institute of Tibetan Plateau Research (LCP201602).

References

Abbot, D. S.,& Tziperman, E. (2008). Sea ice, high-latitude convection, and equable climates. Geophysical

Research Letters, 35(3), 154-175.

An, Z.S., Kutzbach, J.E., Prell, W.L., Porter, S.C.(2001). Evolution of Asian monsoons and phased uplift of the Himalayan Tibetan plateau since Late Miocene times. Nature411, 62–66.

An, Z. (2014). Late Cenozoic Climate Change in Asia. Springer Netherlands.

Ao, H., Roberts, A. P., Dekkers, M. J., Liu, X., Rohling, E. J., & Shi, Z., et al. (2016). Late miocene–plioceneasian monsoon intensification linked to antarctic ice-sheet growth. Earth & Planetary Science Letters,444, 75-87.

Avery, B. W., & Bascomb, C. L. (1974). Soil survey laboratory methods /.

Ballantyne, A. P., Greenwood, D. R., SinningheDamste, J. S., Csank, A. Z., Eberle, J. J., &Rybczynski, N. (2010). Significantly warmer arctic surface temperatures during the pliocene indicated by multiple independent proxies. Geology, 38(7), 603-606.

Brierley, C. M., &Lariviere, J. P. (2009). Greatly expanded tropical warm pool and weakened hadley circulation in the early pliocene. Science,323(5922), 1714-8.

Buggle B, Glaser B, Hambach U, et al.(2011).An evaluation of geochemical weathering indices in loess–paleosol studies[J]. Quaternary International, 240(1–2):12-21.

Chaisson, W. P., &Ravelo, A. C. (2000). Pliocene development of the east-west hydrographic gradient in the equatorial pacific. Paleoceanography, 15(5), 497-505.

Chang, H., An, Z., Wu, F., Jin, Z., Liu, W., & Song, Y. (2013). A Rb/sr record of the weathering response to environmental changes in westerly winds across the tarim basin in the late miocene to the early pleistocene. Palaeogeography Palaeoclimatology Palaeoecology, 386(6), 364-373.

Clift, P. D. (2006). Controls on the erosion of cenozoicasia and the flux of clastic sediment to the ocean. Earth & Planetary Science Letters,241(3–4), 571-580.

Clim. Past Discuss., https://doi.org/10.5194/cp-2018-73
Manuscript under review for journal Clim. Past
Discussion started: 4 July 2018

Clift, P. D., Hodges, K. V., Heslop, D., Hannigan, R., Long, H. V., & Calves, G. (2008). Correlation of himalayan exhumation rates and asian monsoon intensity. Nature Geoscience, 1(12), doi:10.1038/ngeo351.

Clift, P. D., Wan, S., &Blusztajn, J. (2014). Reconstructing chemical weathering, physical erosion and monsoon intensity since 25 ma in the northern south china sea: a review of competing proxies. Earth-Science Reviews, 130(3), 86-102.

Compo, G., Whitaker, J., Sardeshmukh, P., & Mccoll, C. (2013). The quality control system of the 20th century reanalysis dataset. Egu General Assembly, 15.

Ding, Y. (1990). Build-up, air mass transformation and propagation of siberian high and its relations to cold surge in east asia. Meteorology & Atmospheric Physics, 44(1-4), 281-292.

Ding, Z. L., Yang, S. L., Sun, J. M., & Liu, T. S. (2001). Iron geochemistry of loess and red clay deposits in the chinese loess plateau and implications for long-term asian monsoon evolution in the last 7.0 ma. Earth & Planetary Science Letters, 185(1), 99-109.

Driscoll, N. W., & Haug, G. H. (1998). A short circuit in thermohaline circulation: a cause for northern hemisphere glaciation?. Science,282(5388), 436.

Dowsett, H. J., Robinson, M., Haywood, A., Salzmann, U., Hill, D., &Sohl, L., et al. (2010). The prism3d paleoenvironmentalreconstruction. Stratigraphy, 7, 123-139.

Fedorov, A. V., Brierley, C. M., Lawrence, K. T., Liu, Z., Dekens, P. S., & Ravelo, A. C. (2013). Patterns and mechanisms of early pliocene warmth. Nature, 496 (7443), 43.

Fang, X., Li, J., Derbyshire, E., Fitzpatrick, E. A., & Kemp, R. A. (1994). Micromorphology of the beiyuan loess-paleosol sequence in gansu province, china: geomorphological and paleoenvironmental significance. Palaeogeography Palaeoclimatology Palaeoecology, 111(3–4), 289-303.

Fang, X. M., Ono, Y., Fukusawa, H., Pan, B. T., Li, J. J., & Guan, D. H., et al. (1999). Asian summer monsoon instability during the past 60,000 years: magnetic susceptibility and pedogenic evidence from the western chinese loess plateau. Earth & Planetary Science Letters, 168(3–4), 219-232.

Fang, X., Yan, M., Voo, R. V. D., Rea, D. K., Song, C., & Parés, J. M., et al. (2005a). Late cenozoic deformation and uplift of the ne tibetan plateau: evidence from high-resolution magnetostratigraphy of the guide basin, qinghai province, china. Geological Society of America Bulletin,117(9), 1208-1225.

Fang, X., Zhao, Z., Jijun, L. I., Yan, M., Pan, B., & Song, C., et al. (2005b). Magnetostratigraphy of the late cenozoic laojunmiao anticline in the northern qilian mountains and its implications for the northern tibetan plateau uplift. Science in China, 48(7), 1040-1051.

Fang X.M, Wu fuli.(2008). Plio-Pleistocene drying process of Asian inland-sporopollen and salinity records from Yahu section in the central Qaidambasin(in Chinese). Quaternary Sciences 28(5): 874-882

Guo, Z. T., Peng, S. Z., Hao, Q. Z., Biscaye, P. E., & Liu, T. S. (2001). Origin of the miocene–pliocene red-earth formation at xifeng in northern china and implications for paleoenvironments. Palaeogeography Palaeoclimatology Palaeoecology, 170(1–2), 11-26.

Haug, G. H., & Tiedemann, R. (1998). Effect of the formation of the isthmus of panama on atlantic ocean thermohaline circulation. Nature,393(3), 673-676.

Haug, G. H., Tiedemann, R., Zahn, R., &Ravelo, A. C. (2001).Role of panama uplift on oceanic freshwater balance. Geology, 29(3), 207-210.

Haug, G. H., Ganopolski, A., Sigman, D. M., Rosell-Mele, A., Swann, G. E., & Tiedemann, R., et al. (2005). North pacific seasonality and the glaciation of north america 2.7 million years ago. Nature, 433(7028), 821-825.

Huang, R.H., Zhou L.T., & Chen, W. (2003).The progresses of recent studies on the variabilities of the East Asian monsoon and their causes, Adv. Atmos. Sci., 20, 55-69.

Jansen, E., &Sjøholm, J. (1991). Reconstruction of glaciation over the past 6 myr from ice-borne deposits in the norwegian sea. Nature,349(6310), 600-603.

Karas, C., Nürnberg, D., Tiedemann, R., & Garbe-Schönberg, D. (2011). Pliocene climate change of the southwest pacific and the impact of ocean gateways. Earth & Planetary Science Letters, 301(1–2), 117-124.

King, T., 1996. Quantifying non-linearity and geometry in time series of climate. Quaternary Science Reviews 15, 247-266.

Laskar, J. (2004). Long-term solution for the insolation quantities of the earth. Proceedings of the International Astronomical Union, 2(14), 101-106.

Lawrence, K. T., Liu, Z., & Herbert, T. D. (2006). Evolution of the eastern tropical pacific through plio-pleistocene glaciation. Science, 312(5770), 79-83.

Liang, L., Sun, Y., Beets, C. J., Prins, M. A., Wu, F., & Vandenberghe, J. (2013). Impacts of grain size sorting and chemical weathering on the geochemistry of jingyuan loess in the northwestern chinese loess plateau. Journal of Asian Earth Sciences, 69(12), 177-184.

Li, F. J., Rousseau, D. D., Wu, N., Hao, Q., & Pei, Y. (2008). Late neogene evolution of the east asian monsoon revealed by terrestrial mollusk record in western chinese loess plateau: from winter to summer dominated sub-regime. Earth & Planetary Science Letters, 274(3–4), 439–447.

Li, J.J. (1991). The environmental effects of the uplift of the qinghai-xizang plateau. Quaternary Science Reviews, 10(6), 479-483.

Li, J.J., Fang, X., Song, C., Pan, B., Ma, Y., & Yan, M. (2014). Late Miocene–quaternary rapid stepwise uplift of the ne tibetan plateau and its effects on climatic and environmental changes. Quaternary Research,81(3), 400-423.

Li, J. J., Zhou, S. Z., Zhao, Z. J., & Zhang, J. (2015). The qingzang movement: the major uplift of the qinghai-tibetan plateau. Science China Earth Sciences, 58(11), 2113-2122.

Li, J., Ma, Z., Li, X., Peng, T., Guo, B., Zhang, J., ... & Ye, X. (2017). Late Miocene-Pliocene geomorphological evolution of the Xiaoshuizi peneplain in the Maxian Mountains and its tectonic significance for the northeastern Tibetan Plateau. Geomorphology. 295 (2017), 393-405.

Liu, X. M., Rolph, T., An, Z., & Hesse, P. (2003). Paleoclimatic significance of magnetic properties on the red clay underlying the loess and paleosols in china. Palaeogeography Palaeoclimatology Palaeoecology, 199(1), 153-166.

Liu, C. Q., Masuda, A., Okada, A., Yabuki, S., Zhang, J., & Fan, Z. L. (1993). A geochemical study of loess and desert sand in northern china: implications for continental crust weathering and composition. Chemical Geology, 106(3–4), 359-374.

Liu, Q., Jackson, M. J., Yu, Y., Chen, F., Deng, C., & Zhu, R. (2004). Grain size distribution of pedogenic magnetic particles in chinese loess/paleosols. Geophysical Research Letters, 312(22), 359-393..

Liu, Q., Torrent, J., Maher, B. A., Yu, Y., Deng, C., & Zhu, R., et al. (2005). Quantifying grain size distribution of pedogenic magnetic particles in chinese loess and its significance for pedogenesis. Journal of Geophysical Research Atmospheres, 110(B11)

Liu, W., Liu, Z., An, Z., Sun, J., Chang, H., & Wang, N., et al. (2014). Late miocene episodic lakes in the arid tarim basin, western china. Proceedings of the National Academy of Sciences, 111(46), 16292-6

Lu, H., Zhang, F., Liu, X., & Duce, R. A. (2004). Periodicities of palaeoclimatic variations recorded by loess-paleosol sequences in china.Quaternary Science Reviews, 23(18–19), 1891–1900.

Lunt, D. J., Valdes, P. J., Haywood, A., &Rutt, I. C. (2008). Closure of the panama seaway during the pliocene: implications for climate and northern hemisphere glaciation. Climate Dynamics, 30(1), 1-18.

Ma Yuzhen, Fuli, FANG, Xiaomin, Jijun, & Zhisheng, et al. (2005). Pollen record from red clay sequence in the central loess plateau between 8.10 and 2.60 ma. Chinese Science Bulletin, 50(19), 2234-2243.

Mudie, P. J., &Helgason, J. (1983). Palynological evidence for miocene climatic cooling in eastern iceland about 9.8 myr ago. Nature, 303(5919), 689-692.

Nesbitt, H. W., Markovics, G., & Price, R. C. (1980). Chemical processes affecting alkalis and alkaline earths during continental weathering. Geochimica Et Cosmochimica Acta, 44(11), 1659-1666.

Nie, J., Stevens, T., Song, Y., King, J. W., Zhang, R., & Ji, S., et al. (2014). Pacific freshening drives pliocene cooling and asian monsoon intensification. Scientific Reports, 4, 5474-5474.

Raymo, M. E., & Nisancioglu, K. H. (2003). The 41 kyr world: milankovitch's other unsolved mystery. Paleoceanography, 18(1),

Swart, P. K., Lohmann, K. C., Mckenzie, J., & Savin, S. (1993). Influence of Climate on the Formation and Isotopic Composition of Calcretes. Climate Change in Continental Isotopic Records. American Geophysical Union.

Song, C., Fang, X., Li, J., Gao, J., Zhao, Z., & Fan, M. (2001). Tectonic uplift and sedimentary evolution of the jiuxi basin in the northern margin of the tibetan plateau since 13 ma bp. Science China Earth Sciences,44(1), 192-202.

Song, Y., Fang, X., Torii, M., Ishikawa, N., Li, J., &An, Z. (2007). Late neogene rock magnetic record of climatic variation from Chinese eolian sediments related to uplift of the tibetan plateau. Journal of Asian Earth Sciences, 30(2), 324-332.

Sun, D., Bloemendal, J., Rea, D. K., An, Z., Vandenberghe, J., & Lu, H., et al. (2004). Bimodal grain-size distribution of chinese loess, and its palaeoclimatic implications. Catena, 55(3), 325-340.

Sun, J., & Liu, T. (2006a). The age of the taklimakan desert. Science,312(5780), 1612-1621.

Sun, J., & Huang, X. (2006b). Half-precessional cycles recorded in chinese loess: response to low-latitude insolation forcing during the last interglaciation. Quaternary Science Reviews, 25(9–10), 1065-1072.

Sun, J., Liu, W., Liu, Z., Deng, T., Windley, B. F., & Fu, B. (2017). Extreme aridification since the beginning of the pliocene in the tarim basin, western china. Palaeogeography Palaeoclimatology Palaeoecology.

Sun, Y., Lu, H., & An, Z. (2006c). Grain size of loess, palaeosol and red clay deposits on the chinese loess plateau: significance for understanding pedogenic alteration and palaeomonsoon evolution. Palaeogeography Palaeoclimatology Palaeoecology, 241(1), 129-138.

Sun, Y., An, Z., Clemens, S. C., Bloemendal, J., &Vandenberghe, J. (2010). Seven million years of wind and precipitation variability on the chinese loess plateau. Earth & Planetary Science Letters, 297(3–4), 525-535.

Sun, Y., Kutzbach, J., An, Z., Clemens, S., Liu, Z., & Liu, W., et al. (2015). Astronomical and glacial forcing of east asian summer monsoon variability. Quaternary Science Reviews, 115, 132-142.

Tang, H., Micheels, A., Eronen, J., &Fortelius, M. (2011). Regional climate model experiments to investigate the asian monsoon in the late miocene. Climate of the Past, 7(3), 847-868.

Taylor, S. R., Mclennan, S. M., & Mcculloch, M. T. (1983). Geochemistry of loess, continental crustal composition and crustal model ages. Geochimica Et Cosmochimica Acta, 47(11), 1897-1905.

Vandenberghe, J., H. Lu, D. Sun, J. Van Huissteden, and M. Konert (2004), The late Miocene and Pliocene climate in East Asia as recorded by grain size and magnetic susceptibility of the Red Clay

Clim. Past Discuss., https://doi.org/10.5194/cp-2018-73
Manuscript under review for journal Clim. Past
Discussion started: 4 July 2018

Climate of the Past Discussions
Open Access
EGU

deposits (Chinese Loess Plateau), Palaeogeogr. Palaeoclimatol. Palaeoecol., 204, 239–255, doi:10.1016/S0031-0182(03)00729-6.

Wan, S., Tian, J., Steinke, S., Li, A., & Li, T. (2010). Evolution and variability of the east asian summer monsoon during the pliocene: evidence from clay mineral records of the south china sea. Palaeogeography Palaeoclimatology Palaeoecology, 293(1–2), 237-247.

Wang, B., Wu, R., & Fu, X. (2000). Pacific–east asian teleconnection: how does enso affect east asian climate?. Journal of Climate, 13(9), 1517-1536.

Wang, H. B., Chen, F. H., & Zhang, J. W. (2002). Environmental significance of grain size of loess-paleosol sequence in western part of chinese loess plateau. Journal of Desert Research, 22(1), 21-26.

Wang, L. et al. (2006). Palynological evidence for Late Miocene-Pliocene vegetationevolution recorded in the red clay sequence of the central Chinese Loess Plateauand implication for palaeoenvironmental change. Palaeogeogr. Palaeoclimatol. Palaeoecol. 241, 118–128, doi:http://dx.doi.org/10.1016/j.palaeo.2006.06.012

Wara, M. W., Ravelo, A. C., & Delaney, M. L. (2005). Permanent el niño-like conditions during the pliocene warm period. Science, 309(5735), 758-61.

Watanabe, T., Suzuki, A., Minobe, S., Kawashima, T., Kameo, K., &Minoshima, K., et al. (2011). Permanent el nino during the pliocene warm period not supported by coral evidence. Nature, 471(7337), 209-211.

Wu, N., Pei, Y., Lu, H., Guo, Z., Li, F., & Liu, T. (2006). Marked ecological shifts during 6.2–2.4 ma revealed by a terrestrial molluscan record from the chinese red clay formation and implication for palaeoclimatic evolution. Palaeogeography Palaeoclimatology Palaeoecology, 233(3-4), 287-299.

Xia, D., Jia, J., Li, G., Zhao, S., Wei, H., & Chen, F. (2014). Out-of-phase evolution between summer and winter east asian monsoons during the holocene as recorded by chinese loess deposits. Quaternary Research, 81(3), 500-507.

Yang, S., Ding, F., & Ding, Z. (2006). Pleistocene chemical weathering history of asian arid and semi-arid regions recorded in loess deposits of china and tajikistan. Geochimica Et Cosmochimica Acta, 70(7), 1695-1709.

Zachos, J., Pagani, M., Sloan, L., Thomas, E., & Billups, K. (2001).Trends, rhythms, and aberrations in global climate 65 ma to present.Science, 292(5517), 686-93.

Zhang, R., Jiang, D. B., Liu, X. D., & Tian, Z. P. (2012). Modeling the climate effects of different subregional uplifts within the himalaya-tibetan plateau on asian summer monsoon evolution. Science Bulletin, 57(35), 4617-4626.

Zhang, Y. G., Pagani, M., & Liu, Z. (2014). A 12-million-year temperature history of the tropical pacific ocean. Science, 344(6179), 84.

Zheng, H., Mcaulay Powell, C., An, Z., Zhou, J., & Dong, G. (2000). Pliocene uplift of the northern tibetan plateau. Geology, 28(8), 715.

Figures and tables

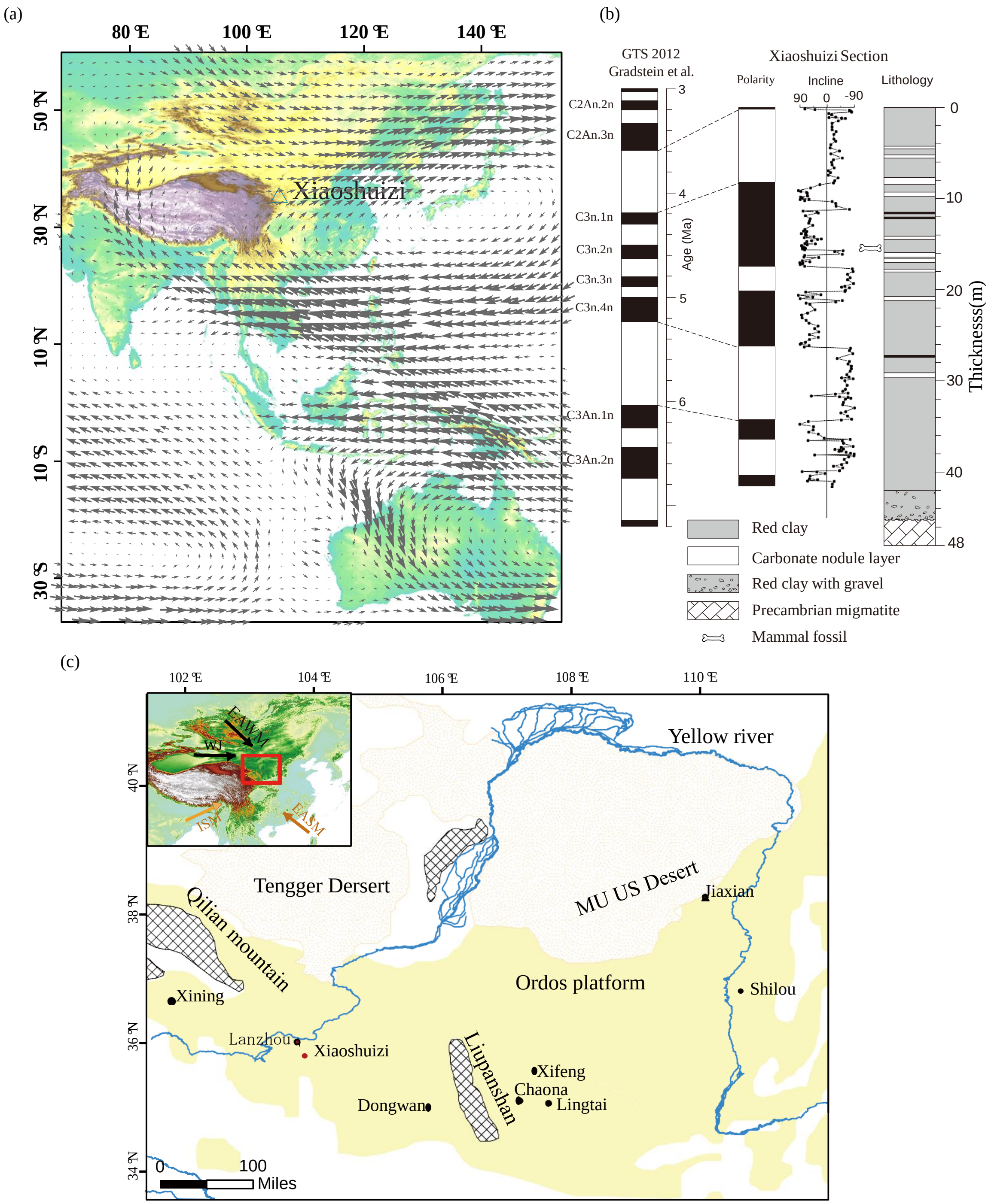

Fig. 1. The location of the study area and atmospheric circulation patterns. (a) 850 mb vector windaveraged from June to August for 1982-2012 based on NOAA Earth System Research Laboratory reanalysis data (Compo et al., 2013). (b) Lithology and magnetostratigraphy of the XSZ drill core (Li et al., 2017). (c) The Chinese Loess Plateau with locations of the studied Xiaoshuizi site and other sections mentioned in the text.

Clim. Past Discuss., https://doi.org/10.5194/cp-2018-73
Manuscript under review for journal Clim. Past
Discussion started: 4 July 2018

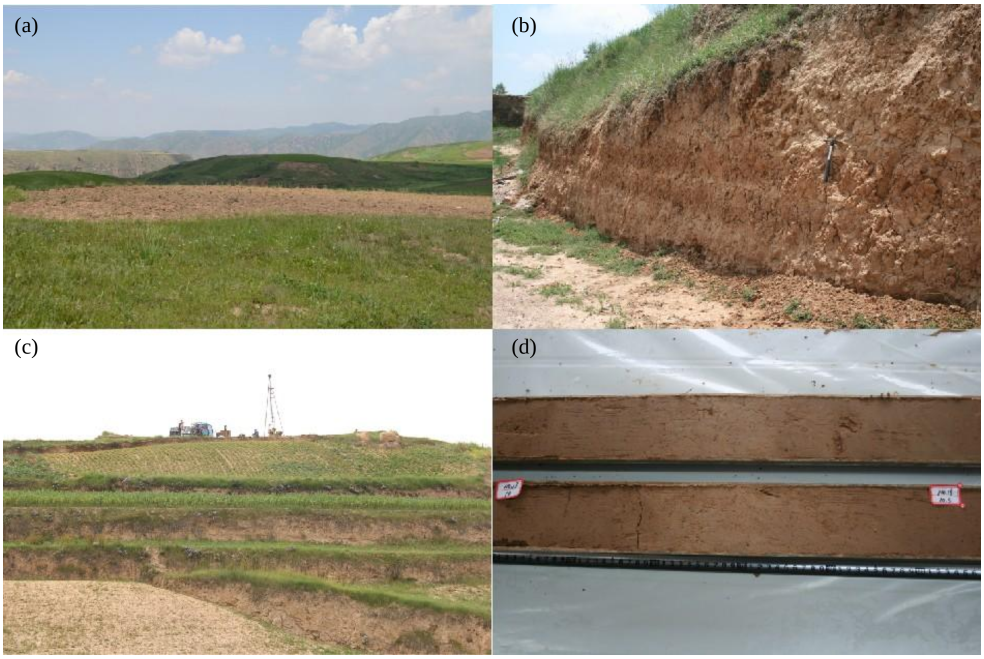

Fig. 2. Photos of the XSZ planation surface and the red clay. (a) XSZ planation surface. (b) Red clay outcrop, XSZ. (c) Position of the XSZ drilling hole. (d) The XSZ drill core.

Clim. Past Discuss., https://doi.org/10.5194/cp-2018-73
Manuscript under review for journal Clim. Past
Discussion started: 4 July 2018

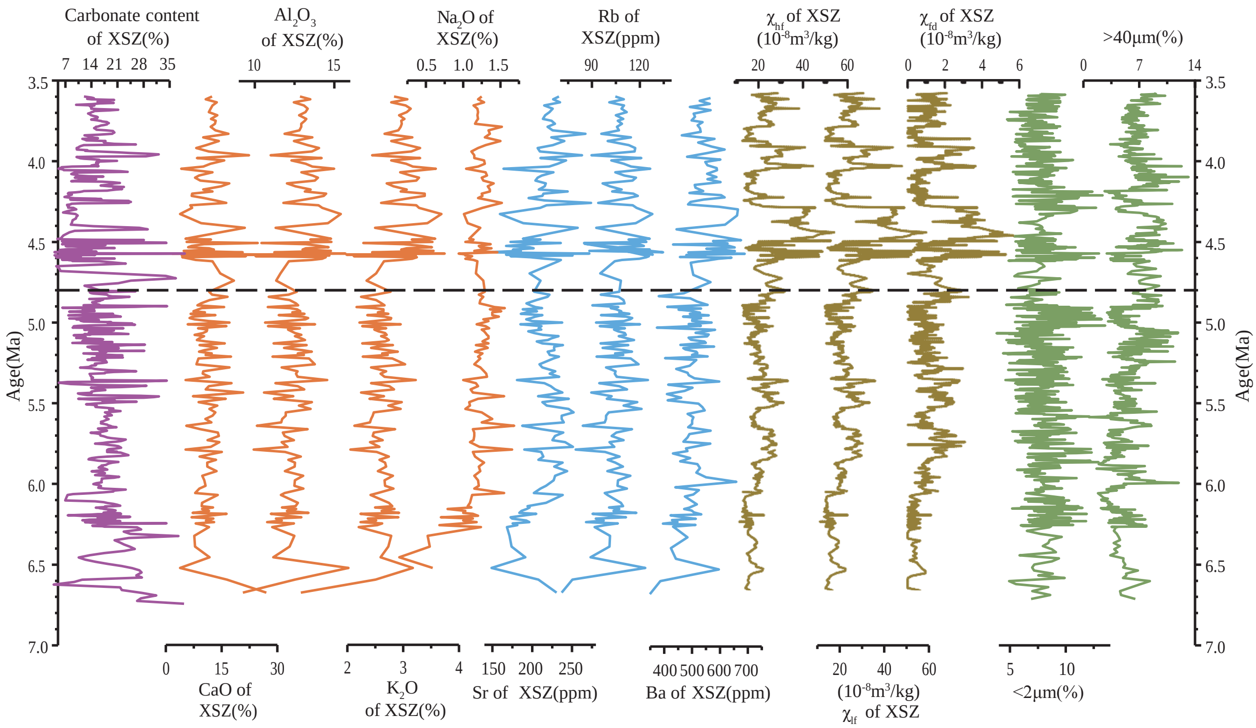

Fig. 3. Variations in carbonate content, major element concentration, minor element concentration, magnetic susceptibility and grain size from the XSZ red clay section, spanning 6.7-3.6 Ma.

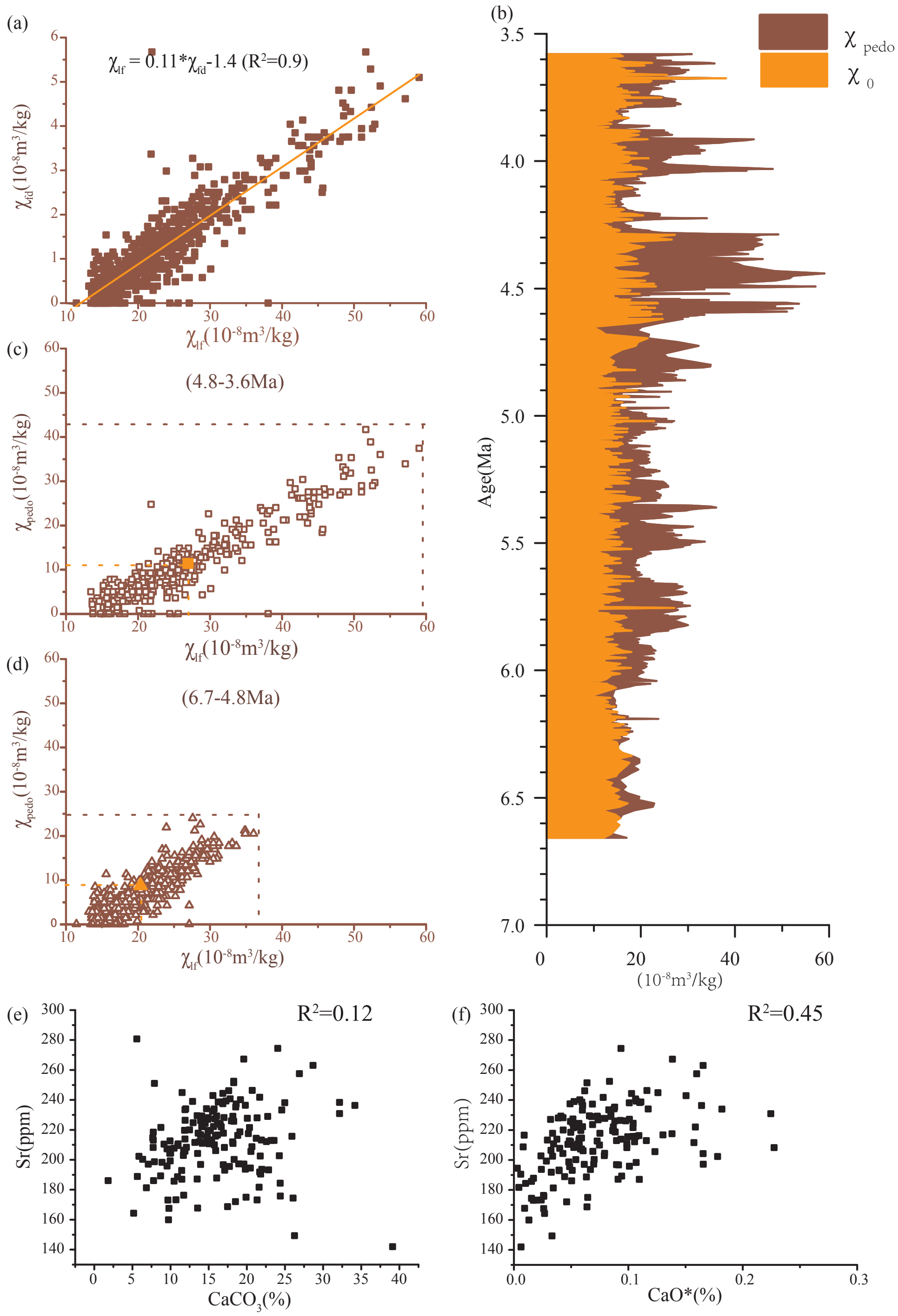

Fig. 4. (a) Scatter plots of χ_{lf} versus χ_{fd}. (b) Separation of χ_{pedo} and χ_0. (c) Scatter plot of χ_{lf} versus χ_{pedo} during 4.8-3.6 Ma. (d) Scatter plot of χ_{lf} versus χ_{pedo} during 6.7-4.8 Ma. (e) Scatterplot of Sr versus $CaCO_3$. (f) Scatter plot of Sr versus CaO*. Solid squares and triangles are the average values during 4.8-3.6 Ma and 6.7-4.8 Ma, respectively. χ_{pedo} is the magnetic susceptibility of pedogenic origin and χ_0 is the magnetic susceptibility of the detrital material.

Clim. Past Discuss., https://doi.org/10.5194/cp-2018-73
Manuscript under review for journal Clim. Past
Discussion started: 4 July 2018

Climate of the Past Discussions
Open Access

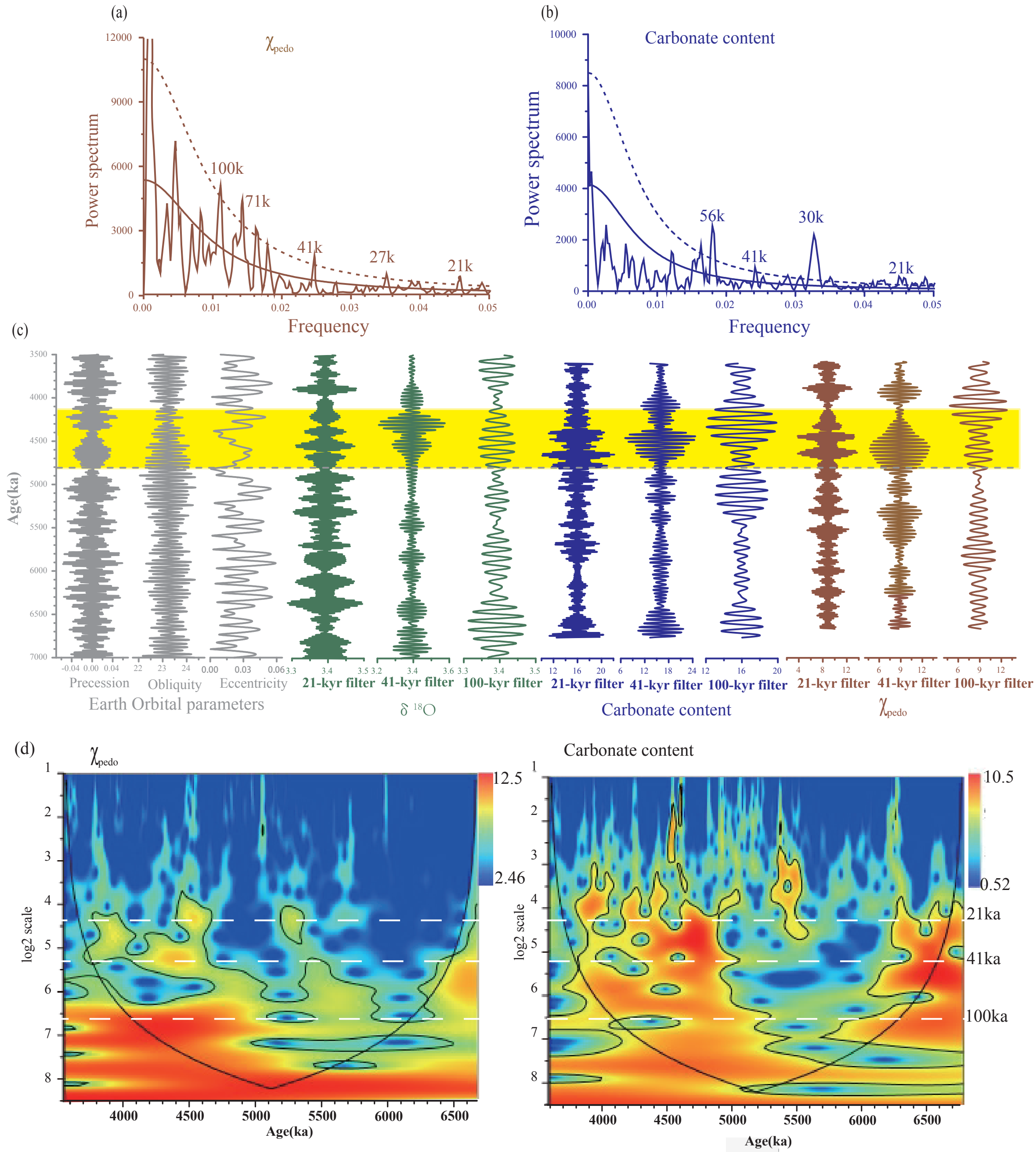

Fig. 5. Spectrum analysis of the red clay. (a) χ_{pedo} and (b) carbonate content(blue) on original paleomagnetism chronology. Dashed lines are 90% confidence limit lines. (c) Comparison of orbital parameters (i.e., eccentricity, obliquity and precession,Laskar et al., 2004) with filtered components of the carbonate content, χ_{pedo} and $\delta^{18}O$ records (Zachos et al.,2001) at the 21-kyr, 41-kyr, and 100-kyr bands. Yellow shading denote the largest amplitude of filtered components of carbonate and χ_{pedo} at the three orbital bands. Dashed lines indicate a large shift in the East Asian monsoon circulation occurred around 4.8 Ma. (d) Results of the wavelet transform of χ_{pedo} and carbonate content time series.

Clim. Past Discuss., https://doi.org/10.5194/cp-2018-73
Manuscript under review for journal Clim. Past
Discussion started: 4 July 2018

Climate of the Past Discussions
Open Access
EGU

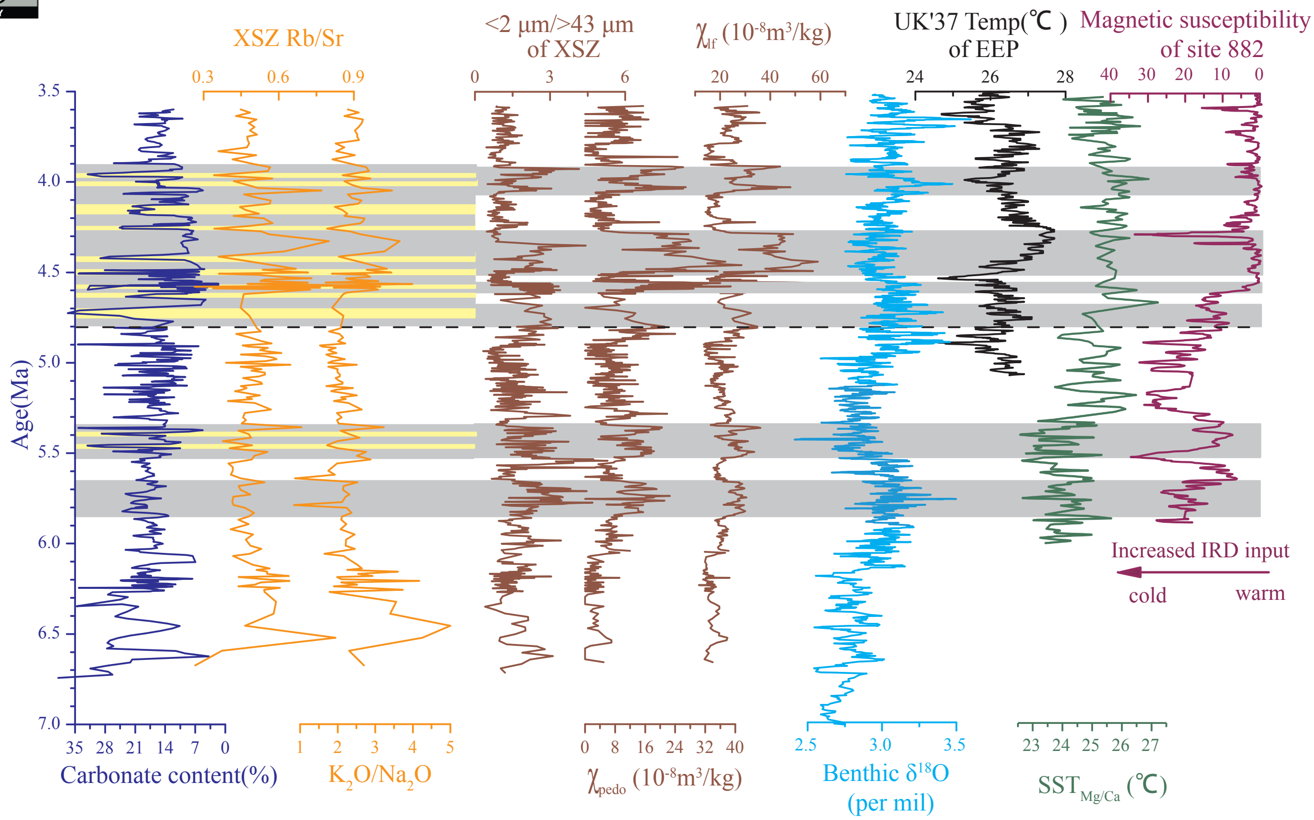

Fig. 6. Temporal evolution of the palaeo-ASM. The dark blue line represents changes in effective precipitation at XSZ, the orange line represents changes in chemical weathering intensity, and the brown lines represent changes in pedogenic intensity. The blue line is the stacked deep-sea benthic foraminiferal oxygen isotope curve compiled from data from DSDP and ODP sites (Zachos et al., 2001). The black line is a reconstruction of sea surface tempeature in the eastern equatorial Pacific (EEP) from ODP Site 846 (Lawrence et al., 2006). Green line is a reconstruction temperature at the edge of warm pool from southwest Pacific Ocean Site 590B (Karas et al., 2011). Purple line is magnetic susceptibility from ODP Site 882 (Haug et al., 2005). Gray shading shows intervals of strong palaeo-ASM and the light-yellow shading shows intervals of carbonate accumulation.

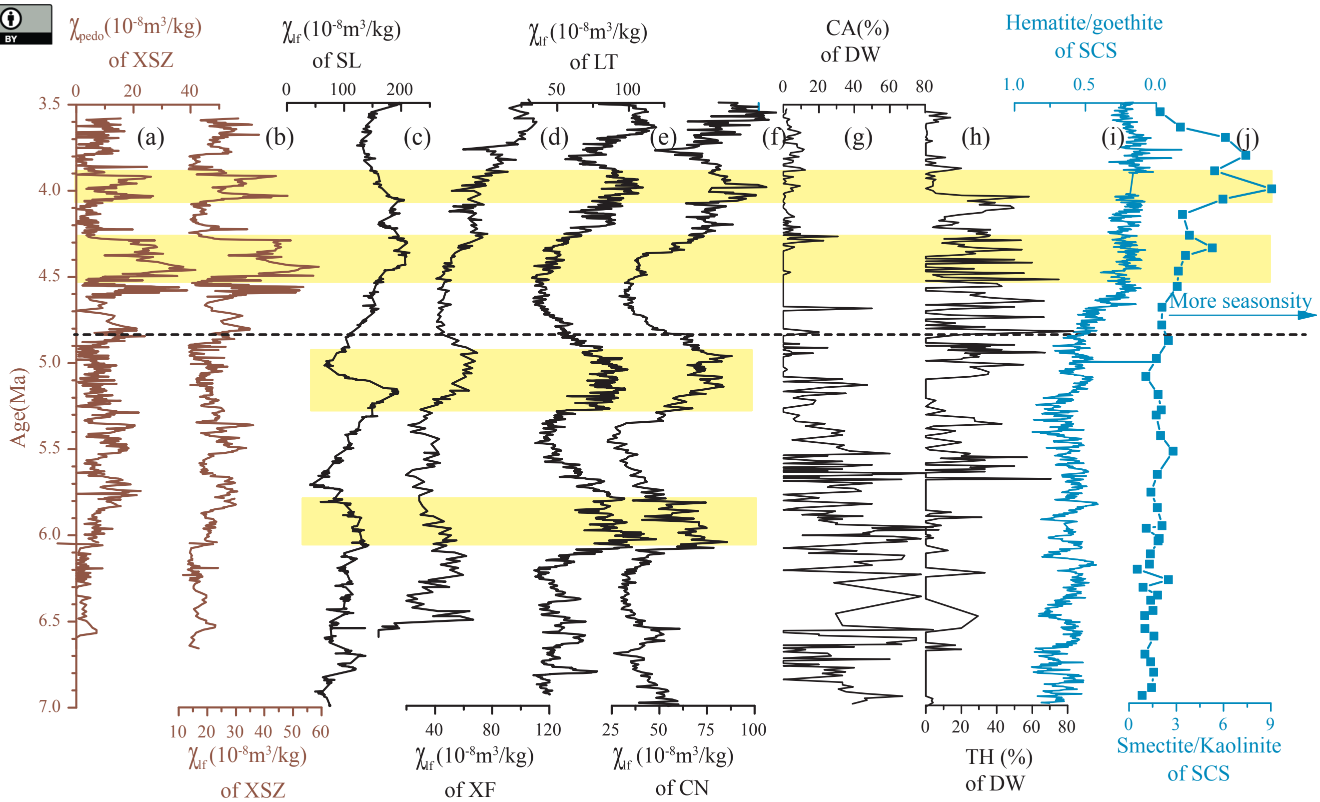

Fig. 7. Comparison of late Miocene-Pliocene paleoclimatic records from Asia. (a-b) χ_{pedo} and χ_{lf} from the XSZ section. (c-f) χ_{lf} record from Shilou (Ao et al., 2016), Xifeng (Guo et al., 2001), Lingtai (Sun et al., 2010) and Chaona (Song et al., 2007). (g-h) Percentages of cold-aridiphilous (CA) mollusk group and thermo-humidiphilous (TH) mollusk group from Donwan(Li et al., 2008), (i) Hematite/goethite ratio from the South China Sea (Clift, 2006). (j) Smectite/Kaolinite ratio from the South China Sea (Wan et al., 2010; Clift et al., 2014).

Climate of the Past Discussions
Open Access

Table 1. major element compositions of XSZ red clay.

Content	SiO_2(%)	Al_2O_3(%)	Fe_2O_3(%)	CaO(%)	MgO(%)
Average	49.16	12.61	5.38	11.36	2.76
6.7-4.8Ma	48.85	12.22	5.18	11.20	3.06
4.8-3.6Ma	49.50	13.22	5.69	11.60	2.30
Content	K_2O(%)	Na_2O(%)	Rb(ppm)	Sr(ppm)	Ba(ppm)
Average	2.76	1.22	106.2	212.8	519.0
6.7-4.8Ma	2.59	1.20	103.9	211.7	494.3
4.8-3.6Ma	3.03	1.23	109.9	214.6	558.0